Nuclear Instruments and Methods in Physics Research A262 (1987) 200–206
North-Holland, Amsterdam

LYRAN: A PROGRAM FOR THE ANALYSIS OF LINAC BEAM DYNAMICS

J.-Q. LU *, I. BEN-ZVI ** and J.G. CRAMER

Nuclear Physics Laboratory GL-10, University of Washington, Seattle, WA 98195, USA

Received 4 March 1987

The FORTRAN program LYRAN has been written for use in analyzing the beam dynamics of superconducting heavy ion linacs. The program is based on the program LYRA developed by A.H. Scholldorf at SUNY Stony Brook, but that original program has been extensively extended, modified, and restructured. LYRAN transports a group of input particles randomly distributed on a selected distribution function through linac elements which include rf accelerating and bunching elements, dipole and quadrupole magnets, electrostatic elements, and drift spaces. Second order corrections to dipole and quadrupole fields are included. A nonlinear optimization routine is incorporated, providing fast and efficient determination of accelerator configurations and parameter settings that provide desired beam properties. Beam envelope plotting is also included to provide a graphic display of beam characteristics.

1. Introduction

The program LYRA [1] was originally written by A.H. Scholldorf in Stony Brook, the State University of New York in 1978 to calculate linac beam lines consisting of SLRs (split loop resonators), drift spaces and quadrupoles. Six-dimensional beam transport was simulated through a sequence of independently phased, nonlinear resonators separated by drift spaces and quadrupoles. The transverse motions were simulated with 4-dimensional transfer matrices coupled by 2-dimensional longitudinal motions. Monte Carlo techniques were used to simulate the evolution of the beam through the sequence of beam elements.

Modifications and improvements to the Stony Brook program LYRA were begun at the University of Washington Nuclear Physics Laboratory in 1984 as a part of the superconducting linac construction project which was begun at that time. These modifications and improvements developed into the new program LYRAN which is described here. LYRAN has been extended to provide 6 (rather than 2) superconducting resonator types and in particular to include descriptions of the two quarter wave resonator designs ($\beta = 0.1$ and 0.2) used in the UW linac. Options for bi-uniform volume distributions and bi-uniform surface distributions in the 6-dimensional beam phase space were added to the code. A "notched" version of the bi-uniform surface distribution (see fig. 1) is also provided to make more apparent the rotation of beam phase space ellipses during transport. Additional accelerator elements were added to the code, including dipole magnets with realistic fringing fields, electrostatic quadrupoles, 3-tube einzel lenses, 3-aperture einzel lenses, 2-tube accelerating lenses, dc accelerating tubes, and charge-changing stripper foils have been put into the program. The second order correction terms for the dipole and quadrupole magnetic elements have also been added. With these additions, a complete accelerator system from ion source to target could be analyzed and optimized.

In the original version of the program the optimization of accelerator configurations and parameters was a serious problem because, aside from linac quadrupole settings, the program had no search capabilities. To speed up the program and provide searching for the desired optical conditions automatically, the following modifications were made: (1) drift space transfer matrices of 6×6 dimensions were incorporated, (2) dipole and quadrupole transfer matrices were enlarged from 4×4 to 6×6 dimensions, (3) a resonator transfer matrix with more accuracy has replaced the old one, (4) the particle ray coordinate vector was enlarged from 4 to 6 dimensions (5) the program was restructured to minimize page faults in the VAX 11/780 operating environment by transporting all rays through one element of the accelerator before moving to the next element, and (6) the beam envelopes both in transverse and longitudinal phase spaces can be plotted out so that the beam dynamics characteristics can be investigated more directly. Finally, (7) the Powell nonlinear pro-

* On leave from Department of Technical Physics, Beijing University, Beijing, P.R. China.

** On leave from Department of Nuclear Physics, The Weizmann Institute of Science, Rehovot 76100, Israel.

0168-9002/87/$03.50

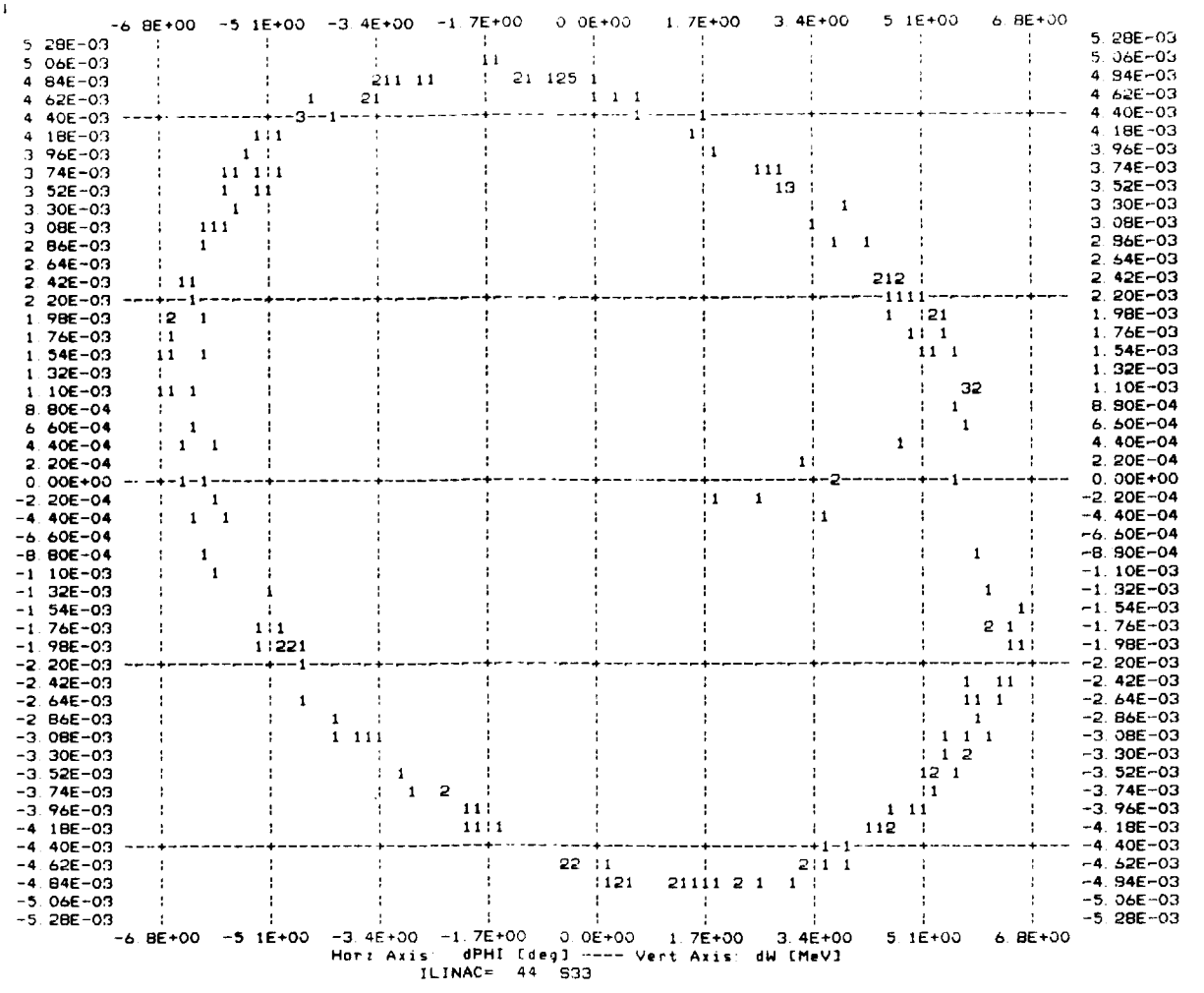

Fig. 1. A phase ellipse in dW–$d\phi$ space generated as a bi-uniform surface distribution. Note the "notch" used to monitor rotation of the phase ellipse.

gramming method [3] was incorporated into the program to search for the desired optical conditions.

2. Optimizing calculations

The Powell nonlinear optimizing method is used in LYRAN to search automatically for the required optical conditions. The main reasons we use this method are: (1) it is a type of conjugational gradient method which provides fast convergence; (2) one does not need to calculate the derivatives of the object function, making this algorithm convenient to use when the object function is implicit and complex; (3) the number of optical boundary conditions does not necessarily have to be equal to the number of variables in the optimization.

The object function $F_{\min}$ is minimized by the search procedure. It is created from the specified optical conditions and requirements and expressed as:

$$F_{\min}\sum\left[\frac{f_i(x_1, x_2, \cdots, x_m) - f_{i0}}{\epsilon_i}\right]^2, \tag{1}$$

where f_i $(i = 1, 2, \cdots, n)$ is an optical condition, which is one either of the transfer matrix elements or of the beam σ matrix elements, x_j $(j = 1, 2, \cdots, m)$ is a variable which stands for the focusing strength of quadrupoles, electrostatic lenses or resonator fields, f_{i0} is the desired value of f_i, ϵ_i is the desired accuracy (weight factor).

3. Beam profile calculations and plotting

The original program LYRA provided line printer plots of beam ellipses in x–x', y–y', x–y, and in

$\Delta\phi$–ΔE spaces (fig. 1). The program was designed to transport each ray of the beam phase space successively through all elements of the linac, recording the position of the ray in arrays representing selected points in the path. This method, which was originally used by Scholldorf very effectively in a large mainframe computer system, had the disadvantage in the VAX environment that it randomly accesses many large arrays, producing much page faulting and degraded program performance.

For LYRAN this beam transport strategy was changed in two ways. First the transport algorithm was modified so that all rays were transported together through one linac element at a time. This dramatically reduced page faulting in the VAX. Further, with this procedure the envelope and moments of the beam could be calculated at each transport point. This made it straightforward to provide new plots of beam envelopes in x–y and $\Delta\phi$–ΔE spaces. Plotting of these beam envelopes provides a direct indication of beam quality in both transverse and longitudinal phase spaces during transport through the accelerator (fig. 2).

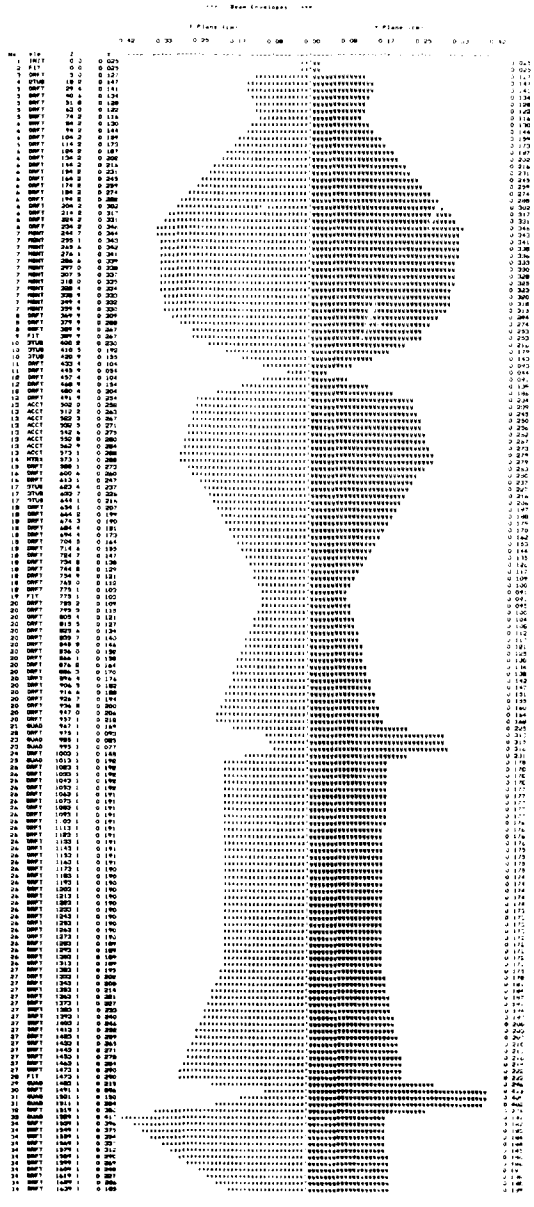

Fig. 2. Beam envelopes in x-plane (left) and y-plane (right).

The program LYRAN has been in use in more or less the present form for about four months. We have used it to develop a mathematical model of the UW superconducting linac and its tandem Van de Graaff injector. As we gain operating experience with this new facility, this model will be refined so that it can be used to rapidly develop beam solutions and operating parameters and can be used to reconfigure the accelerator system in response to changes in operating conditions, particularly resonator performance. In the near future an interface between LYRAN and the control system of the linac will be created so that calculated operating parameters based on the LYRAN model of the machine can be directly employed to set power supplies and control parameters.

Acknowledgements

The authors would like to thank A.H. Scholldorf, J. Haastedt, and J.M. Brennan of the linac group at SUNY Stony Brook for their assistance in providing advice and software which provided the basis for our development of beam dynamics calculations for our linac project. We would also like to acknowledge valuable contributions to the work described here which were provided by Dr. D.W. Storm, director of the UW linac project.

Appendix

Beam dynamics formulas

In this Appendix we describe the equations, taken from standard sources, which are used as the six-dimensional transport matrices for LYRAN.

(1) Description of beam phase space

The coordinate vector of a particle ray is expressed by

$$\boldsymbol{X}(x,\ x',\ y,\ y',\ \Delta\phi,\ \Delta E). \tag{2}$$

x is the particle position off-axis in one transverse direction, $x' = \mathrm{d}x/\mathrm{d}z$, y is the particle position off-axis

in another transverse direction, $y' = \mathrm{d}y/\mathrm{d}z$, $\Delta\phi$ is the phase angle relative to a standard particle, and ΔE is the energy relative to a standard particle.

To first order, the actions of a physical element on the particles are expressed by a transfer matrix **M**. After each element, the new coordinates of a particle ray are

$$\boldsymbol{X} = \mathbf{M}\boldsymbol{X}_0. \tag{3}$$

At the beginning of each fitting procedure, the initial beam σ matrix was obtained from the statistics of the ensemble of transported particles. The new beam matrix σ was then obtained from the equation:

$$\sigma = \mathbf{M}\sigma_0\mathbf{M}^{\mathrm{T}}. \tag{4}$$

Here **M** is the transfer matrix of a beam line section, and $\mathbf{M}^{\mathrm{T}}$ is its transpose.

(2) Accelerator element transfer matrices

(a) Drift spaces:

$$\begin{bmatrix} 1 & L & 0 & 0 & 0 & 0 \\ 0 & 1 & 0 & 0 & 0 & 0 \\ 0 & 0 & 1 & L & 0 & 0 \\ 0 & 0 & 0 & 1 & 0 & 0 \\ 0 & 0 & 0 & 0 & 1 & D \\ 0 & 0 & 0 & 0 & 0 & 1 \end{bmatrix}, \tag{5}$$

where L is the drift distance,

$$D = -\frac{\omega}{c}\frac{L}{E_r\beta^3\gamma},$$

ω is the cycle frequency, c is the velocity of light, E_r is the particle rest energy, βc is the particle velocity, and $\gamma = (1-\beta^2)^{-1/2}$.

(b) Dipole magnets:

$$\begin{bmatrix} \cos\phi & R\sin\phi & 0 & 0 & 0 & \frac{R}{2E_s}(1-\cos\phi) \\ -\sin\phi/R & \cos\phi & 0 & 0 & 0 & \frac{1}{2E_s}\sin\phi \\ 0 & 0 & 1 & R\phi & 0 & 0 \\ 0 & 0 & 0 & 1 & 0 & 0 \\ \sin\phi & \frac{\omega R}{v_s}(1-\cos\phi) & 0 & 0 & 1 & -\frac{\omega R}{2E_s}\sin\phi \\ 0 & 0 & 0 & 0 & 0 & 1 \end{bmatrix}, \tag{6}$$

where ϕ is the bending angle, R is the curvature radius, E_s is the standard particle energy, v_s is the standard particle velocity, and ω is the cycle frequency.

(c) Fringing fields:

$$\begin{bmatrix} 1 & 0 & 0 & 0 & 0 & 0 \\ \frac{\tan\beta}{R} & 1 & 0 & 0 & 0 & 0 \\ 0 & 0 & 1 & 0 & 0 & 0 \\ 0 & 0 & -\frac{\tan(\beta-\phi)}{R} & 1 & 0 & 0 \\ 0 & 0 & 0 & 0 & 1 & 0 \\ 0 & 0 & 0 & 0 & 0 & 1 \end{bmatrix} \tag{7}$$

where β is the fringing angle, R is the curvature radius of the magnet, and

$$\phi = K_1\left(\frac{g}{R}\frac{1+\sin^2\beta}{\cos\beta}(1-K_1K_2)\left(\frac{g}{R}\right)\tan\beta\right)$$

(see ref. [4]).

(d) Magnetic and electric quadrupoles:

$$\begin{bmatrix} \cos(\omega l) & \frac{1}{\omega}\sin(\omega l) & 0 & 0 & 0 & 0 \\ -\omega\sin(\omega l) & \cos(\omega l) & 0 & 0 & 0 & 0 \\ 0 & 0 & \cosh(\omega l) & \frac{1}{\omega}\sinh(\omega l) & 0 & 0 \\ 0 & 0 & \omega\sinh(\omega l) & \cosh(\omega l) & 0 & 0 \\ 0 & 0 & 0 & 0 & 1 & D \\ 0 & 0 & 0 & 0 & 0 & 1 \end{bmatrix}, \tag{8}$$

where l is the pole length, $\omega^2 = G/(BR)$ for magnetic quadrupoles, $\omega^2 = V/(UR_0^2)$ for electrostatic quadrupoles, G is the magnetic field gradient, BR is the particle magnetic rigidity, V is the voltage on the pole, U is the normalized potential of the particle, R_0 is the aperture radius of the quadrupole, and D is the same as in the drift space matrix.

(e) Second order terms of dipoles and quadrupoles:

The option of performing second order calculations for dipoles and quadrupoles has been put into the program.

$$x_i = \sum R_{ij}x_j^0 + \sum T_{ijk}x_j^0x_k^0, \quad (i, j, k) = 1, 6, \tag{9}$$

where R_{ij} is the transfer matrix of first order. T_{ijk} denotes second order terms [5,6].

(f) Resonator gaps:

Ignoring the second and higher order terms of x, x', y, y', $\Delta\phi$ and ΔE in the formulas of ref. [2], we get the following linear transfer matrix of resonator gaps:

$$\mathbf{M} = \mathbf{M}[i, j] \qquad i, j = 1, 6, \tag{10}$$

where

$$M_{11} = 1 - \frac{\alpha}{2}\left(T_k\frac{k}{\gamma^3} + \frac{T}{\gamma}\right)\cos\phi,$$

$$M_{12} = -\frac{\alpha}{2}T_{kk}\frac{k}{\gamma^3}\sin\phi,$$

$$M_{21} = -\frac{1}{2}\frac{\alpha k}{\gamma^3}T\sin\phi,$$

$$M_{22} = 1 - \frac{\alpha}{\gamma}\left(\frac{1}{\gamma^2} + \frac{\beta^2}{2}\right)T\cos\phi,$$

$$M_{33} = M_{11},$$

$$M_{34} = M_{12},$$

$$M_{43} = M_{21},$$

$$M_{44} = M_{22},$$

$$M_{55} = 1 + \frac{\alpha k T_k}{\gamma^3}\cos\phi,$$

$$M_{65} = -QVT\sin\phi,$$

and

$M_{66} = 1$.

The unlisted matrix elements are all zero and Q is the charge state, V is the voltage over the gap, $\alpha = QV/2E_s$, E_s is the energy of standard particle, $k = \omega/v_s$, v_s is velocity of standard particle, and T, T_k and T_{kk} = transit time factor and its first and second order derivatives, respectively.

When the program is searching for the required optical conditions, the above transfer matrix together with the matrices of other elements are used to get the new beam σ matrix. Conditions on either the matrix elements of **M** or of σ can be used as search criteria. This was discussed in section 2 above. After the optimizing procedures, individual particle rays will be calculated in the nonlinear approximations.

(g) Transfer matrices of electrostatic lenses:

It is usual in calculating beam transport with electrostatic lenses to use empirical data given in the literature [7–10]. However, this is inconvenient in the optimization of optical conditions. To avoid this inconvenience we have included direct calculations of transport matrices for electrostatic elements to the program LYRAN. The transfer matrices are calculated from the potential distributions of these lenses, as discussed below.

We use the following potential distributions:

$$\phi(z) = V_2 + \frac{V_2 - V_1}{2\omega s} \times \ln\left[\frac{\cosh(2\omega z) + \cosh(2\omega(a+s))}{\cosh(2\omega z) + \cosh(2\omega a)}\right], \quad (11)$$

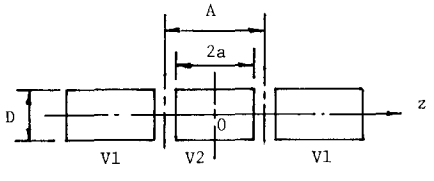

Fig. 3. Three-tube einzel lens.

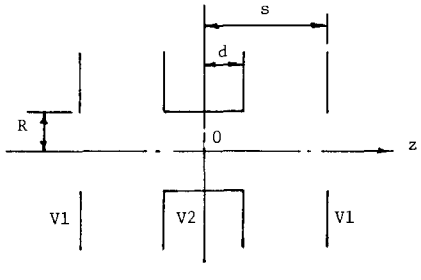

Fig. 4. Three-aperture einzel lens.

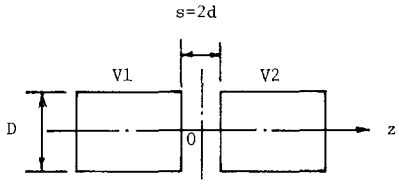

Fig. 5. Two-tube accelerating lens.

for 3-tube einzel lenses [9] (fig. 3), where $\omega = 1.31835$,

$$\phi(z) = V_1 - \frac{V_1 - V_2}{\pi(s-d)}\left[(z+s)\tan^{-1}\frac{(z+s)}{R} + (z-s)\tan^{-1}\frac{(z-s)}{R} - (z+d)\tan^{-1}\frac{(z+d)}{R} - (z-d)\tan^{-1}\frac{(z-d)}{R}\right], \quad (12)$$

for 3-aperture einzel lenses [11] (fig. 4), and

$$\phi(z) = \frac{V_1 + V_2}{2}\left[\left(\frac{V_2}{V_1} + 1\right) + \left(\frac{V_2}{V_1} - 1\right)\frac{1}{2\omega d}\ln\frac{\cosh\omega(z+d)}{\cosh\omega(z-d)}\right], \quad (13)$$

for 2-tube accelerating lenses [8] (fig. 5).

The transfer matrix of dc accelerating tubes with uniform fields is calculated differently (fig. 6). The matrix of the entrance aperture is

$$\begin{bmatrix} 1 & 0 \\ -\dfrac{\eta^2 - 1}{4L\xi_1} & 1 \end{bmatrix}, \quad (14)$$

where $\eta = (V_2/V_1)^{1/2}$, R is the radius of the entrance and exit apertures, L is the length of the tube, and $\xi_1 = 1 + (R/\pi L)(\omega^2 - 1)$.

For the exit aperture we have

$$\begin{bmatrix} 1 & 0 \\ \dfrac{\eta^2 - 1}{4L\eta_2\xi_2} & 1 \end{bmatrix}, \quad (15)$$

where $\xi_2 = 1 - (R/\pi L)(1 - 1/\eta^2)$.

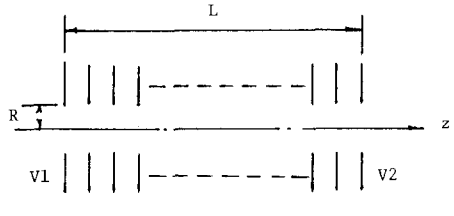

Fig. 6. Dc accelerating tube.

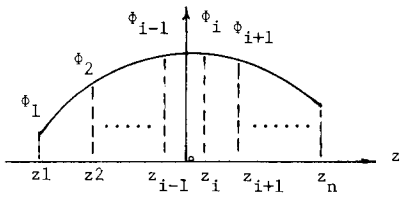

Fig. 7. Potential distribution.

Usually, $R/L \ll 1$ and η is very large, therefore $\xi_2 \cong 1$.

The transfer matrix of the uniform accelerating field is

$$\begin{bmatrix} 1 & \dfrac{2L}{\eta+1} \\ 0 & \dfrac{1}{\eta} \end{bmatrix}. \tag{16}$$

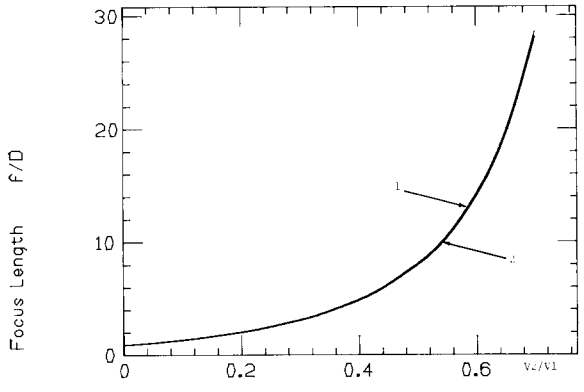

Fig. 8. Three-tube einzel lens (with $A/D = 1.0$): (1) from ref. [7], (2) calculated by program LYRAN.

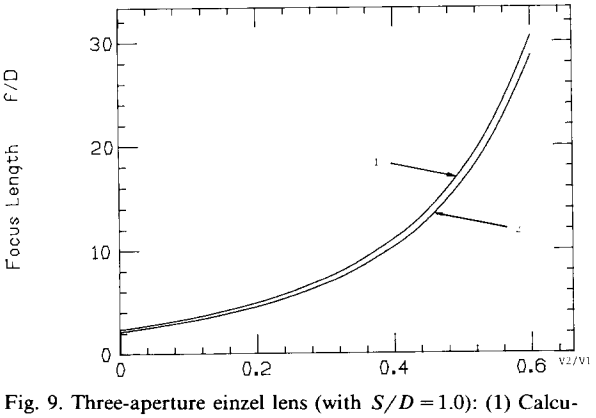

Fig. 9. Three-aperture einzel lens (with $S/D = 1.0$): (1) Calculated by program LYRAN, (2) from ref. [7].

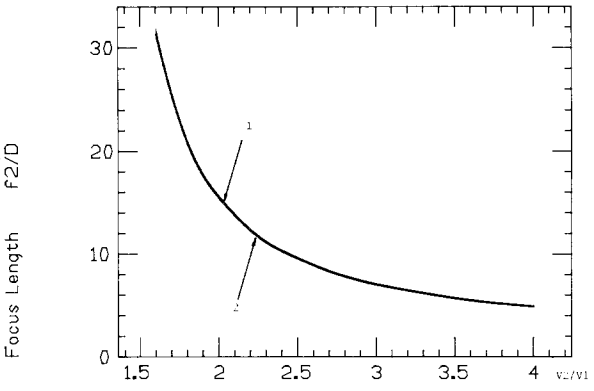

Fig. 10. Two-tube einzel (with $G/D = 1.0$): (1) from ref. [7], (2) calculated by program LYRAN.

Therefore, the total matrix of an accelerating tube is

$$\mathbf{M}_T = \mathbf{M}_3\mathbf{M}_2\mathbf{M}_1 = \begin{bmatrix} \dfrac{2\xi_1 + 1 - \eta}{2\xi_1} & \dfrac{2L}{\eta+1} \\ \dfrac{(\eta^2-1)[2\xi_1 - \eta(2\xi_2+1)+1]}{8\xi_1\xi_2\eta^2 L} & \dfrac{2\xi_2\eta + \eta - 1}{2\xi_2\eta^2} \end{bmatrix}. \tag{17}$$

(h) Potential distributions of electrostatic lenses:

Suppose we know the potential distributions of the electrostatic lenses as shown in eqs. (12), (13) and (14). The transfer matrices are calculated from these analytical expressions.

The effective length of a lens is divided into N small intervals (see fig. 7). Each point z_i is considered as a thin lens, and its matrix is

$$\begin{bmatrix} 1 & 0 \\ -\dfrac{\eta_i\eta_{i+1} - 2\eta_i + 1}{4d_i\eta_i} & 1 \end{bmatrix}, \tag{18}$$

where

$$\eta_i = \phi_i/\phi_{i-1}, \quad d_i = z_i - z_{i-1}.$$

The interval from z_{i-1} to z_i is considered as a uniform accelerating field with matrix

$$\begin{bmatrix} 1 & \dfrac{2d_i}{1+\eta_i^{1/2}} \\ 0 & \dfrac{1}{\eta_i^{1/2}} \end{bmatrix}. \tag{19}$$

The calculated focal lengths are very close to the data listed in ref. [7] and shown in figs. 8–10.

References

[1] A.H. Scholldorf, PhD Thesis, SUNY Stony Brook, the State University of New York (1983).

[2] I. Ben-Zvi and Z. Segalov, Part. Accel. 10 (1979) 31.
[3] D.M. Himmelblau, Applied Nonlinear Programming (McGraw–Hill, New York, 1972).
[4] A. Septier, ed., Focusing of Charged Particles, vol. 2 (Academic Press, New York, 1967).
[5] R.H. Helm, SLAC Report no. 24 (1963).
[6] K.L. Brown, SLAC Report no. 75 (1967).
[7] E. Harting and F.H. Read, Electrostatic Lenses (Elsevier Amsterdam, Oxford, New York, 1976).
[8] A.B. El-Kareh and C.J. El-Kareh, Electron Beams, Lenses and Optics (Academic Press, New York, 1970).
[9] A. Adams and F.H. Read, J. Phys. E5 (1972) 150.
[10] A.B. El-Kareh, J. Appl. Phys. 42 (1971) 1870.
[11] P. Grivet, Electron Optics (Pergamon, New York, 1965).